Amino Acids (2011) 40:809–818
DOI 10.1007/s00726-010-0698-9

ORIGINAL ARTICLE

O-GlcNAcylation of tubulin inhibits its polymerization

Suena Ji · Jeong Gu Kang · Sang Yoon Park · JooHun Lee · Young J. Oh · Jin Won Cho

Received: 8 April 2010 / Accepted: 13 July 2010 / Published online: 28 July 2010

Abstract The attachment of *O*-linked *β*-*N*-acetylglucosamine (*O*-GlcNAc) to proteins is an abundant and reversible modification that involves many cellular processes including transcription, translation, cell proliferation, apoptosis, and signal transduction. Here, we found that the *O*-GlcNAc modification pattern was altered during all-*trans* retinoic acid (tRA)-induced neurite outgrowth in the MN9D neuronal cell line. We identified several *O*-GlcNAcylated proteins using mass spectrometric analysis, including α- and *β*-tubulin. Further analysis of α- and *β*-tubulin revealed that *O*-GlcNAcylated peptides mapped between residues 173 and 185 of α-tubulin and between residues 216 and 238 of *β*-tubulin, respectively. We found that an increase in α-tubulin *O*-GlcNAcylation reduced heterodimerization and that *O*-GlcNAcylated tubulin did not polymerize into microtubules. Consequently, when *O*-GlcNAcase inhibitors were co-incubated with tRA, the extent of neurite outgrowth was decreased by 20% compared to control. Thus, our data indicate that the *O*-GlcNAcylation of tubulin negatively regulates microtubule formation.

Keywords *O*-GlcNAc · Tubulin · Microtubule · Neuron · Neurite

S. Ji · J. G. Kang · S. Y. Park · J. Lee · Y. J. Oh · J. W. Cho
Department of Biology, Yonsei University,
Seoul 120-749, Korea

J. W. Cho (✉)
Department of Integrated OMICS for Biomedical Sciences,
Graduate School, Yonsei University, Seoul 120-749, Korea
e-mail: chojw311@yonsei.ac.kr

Abbreviations

O-GlcNAc	*O*-Linked *β*-*N*-acetylglucosamine
tRA	All-*trans* retinoic acid
PTM	Post-translational modification
MAP	Microtubule-associated protein
OGT	*O*-GlcNAc transferase
OGA	*O*-GlcNAcase
NButGT	1,2-Dideoxy-2′-propyl-α-D-glucopyranoso[2,1-d]-Δ2-thiazoline
PUGNAc	*O*-(2-Acetamido-2-deoxy-D-glycopyranosylidene)amino-*N*-phenylcarbamate
ESI	Electrospray ionization
2-DE	Two-dimensional electrophoresis
sWGA	Succinylated wheat germ agglutinin
CBB	Coomassie Brilliant Blue
IgG HC	Immunoglobulin heavy chain

Introduction

Microtubules are major elements of the cytoskeleton that play essential roles in diverse cellular functions, including vesicular trafficking, cytoplasmic organization, maintenance of cell shape and polarity, and cell division (Westermann and Weber 2003; Verhey and Gaertig 2007; Hammond et al. 2008). The basic building blocks of microtubules are α/*β*-tubulin heterodimers and their polymerization is both highly dynamic and tightly regulated. The specific function of microtubules is regulated through their association with various regulatory proteins, the differential expression of tubulin isotypes, and post-translational modifications (PTMs). Microtubule-associated proteins (MAPs) bind to

soluble α/β-tubulin heterodimers or microtubule surfaces. The expression levels of tubulin isotypes vary and depend on specific cell types or developmental stages. Both α- and β-tubulin subunits are subjected to diverse PTMs including acetylation, tyrosination, detyrosination, polyglutamylation, and polyglycylation.

The attachment of *O*-GlcNAc on serine/threonine residues of nuclear and cytoplasmic proteins is one such PTM (Hart et al. 2007). The addition and removal of *O*-GlcNAc on proteins are catalyzed by *O*-GlcNAc transferase (OGT) and *O*-GlcNAcase (OGA), respectively. OGT uses uridine 5′-diphospho-*N*-acetylglucosamine (UDP-GlcNAc) as a donor sugar, which is synthesized from glucose through the hexosamine biosynthetic pathway (Love and Hanover 2005). In addition, *O*-GlcNAc modifications are dynamically regulated in response to stress and nutrients (Marshall et al. 2004; Zachara et al. 2004; Kang et al. 2009; Yang et al. 2010).

Various proteins are known to be *O*-GlcNAcylated, including the nuclear pore complex, transcription factors, RNA-binding proteins, kinases, cytoskeletal proteins, and metabolic enzymes (Lubas et al. 1995; Wells et al. 2002; Hart et al. 2007). Cytoskeletal proteins, which are known to be modified by *O*-GlcNAc, include cytokeratins (Chou et al. 1992; Ku and Omary 1994), vimentin (Wang et al. 2007; Slawson et al. 2008), MAP2 and -4 (Ding and Vandre 1996; Khidekel et al. 2004; Liu et al. 2004), and tau (Arnold et al. 1996). *O*-GlcNAcylation sites have been identified in some cases, but their functions are still unclear. In addition, α- and β-tubulin have been reported to undergo *O*-GlcNAcylation (Walgren et al. 2003; Wang et al. 2007); however, direct evidence for this modification on tubulin is insufficient and the function of tubulin *O*-GlcNAcylation is not known.

MN9D is a dopaminergic neuronal cell line established by the immortalization of mouse embryonic mesencephalic neurons by somatic cell fusion with neuroblastoma cells (N18TG2; Choi et al. 1991). MN9D cells have immature neuronal cell morphology, and, under certain conditions such as all-*trans* retinoic acid (tRA) treatment, these cells can begin neuronal cell differentiation and sprout neurites (Castro et al. 2001). Neurite outgrowth depends on both cytoskeletal organization and dynamics (Gordon-Weeks 2004; Conde and Caceres 2009). Whereas the actin cytoskeleton plays a crucial role in both filopodia and lamellipodia at growing tip of neurites, microtubules are reorganized into a bundle structure, which is required for neurite extension (Mandell and Banker 1995). In polarizing neuronal cells, these microtubule polymers form at the centriole in the cell body and are transported to neurites; simultaneously, tubulin polymerization occurs at the plus ends of the microtubules in the growing tips (Baas 1997).

Here, we identified *O*-GlcNAcylated proteins from MN9D neuronal cells. We found that α- and β-tubulin were modified with *O*-GlcNAc, and *O*-GlcNAcylated tubulin peptides were analyzed by electrospray ionization (ESI) Q-TOF. In addition, α-tubulin *O*-GlcNAcylation negatively regulated tubulin dimerization and *O*-GlcNAcylated α- and β-tubulin did not polymerized into microtubules. Furthermore, an increase in intracellular *O*-GlcNAcylation reduced neurite outgrowth.

Materials and methods

Reagents and DNA plasmids

The following primary antibodies were used: anti-*O*-GlcNAc (CTD110.6, Covance, Emeryville, CA); mouse monoclonal anti-α-tubulin (DM1A, Sigma, St Louis, MO); mouse monoclonal anti-β-tubulin (TUB 2.1, Sigma); mouse monoclonal anti-FLAG (F 3165, Sigma); rabbit polyclonal anti-FLAG (F 7425, Sigma); mouse monoclonal anti-Myc (sc-40, Santa Cruz Biotechnology, Santa Cruz, CA); and rabbit polyclonal anti-Myc (sc-789, Santa Cruz Biotechnology). Both α- and β-tubulin DNA constructs were prepared by polymerase chain reaction (PCR) using cDNA from MN9D cells and tubulin isotype-specific primers. Four α-tubulin isotypes (TA1, NP_035783; TA1B, NP_035784; TA1C, NP_033474; and TA4, NP_033473) were cloned into the *Hin*dIII and *Xba*I sites of the p3XFLAG-CMV-7.1 vector (Sigma) and four β-tubulin isotypes (TB2B, NP_076205; TB2C, NP_666228; TB3, NP_075768; and TB6, NP_080749) were cloned into the *Xho*I and *Xba*I sites of the pcDNA3.1-mycHis vector (Invitrogen). Sequences of all plasmids were confirmed by DNA sequencing. The mammalian expression vector encoding an untagged form of OGT, pCMV-OGT, was used for OGT over-expression in HEK293 cells.

Cell culture and drug treatment

MN9D cells were plated onto 25 μg/ml poly-D-lysine-coated 100-mm dishes and maintained in Dulbecco's modified Eagle's medium (DMEM) supplemented with 10% fetal bovine serum (FBS) and 1% penicillin/streptomycin in 10% CO_2 at 37°C. Cells were treated with 10 μM tRA (Sigma, St Louis, MO) and OGA inhibitors, PUGNAc (Toronto Research Chemicals, Ontario, Canada) or NButGT (kindly provided by Dr. Kwan Soo Kim, Yonsei University, Seoul, Korea), both 100 μM. HEK293 cells were maintained in DMEM supplemented with 10% FBS and 1% penicillin/streptomycin in 5% CO_2 at 37°C. Cells were transfected with DNA constructs using Lipofectamine

2000 (Invitrogen, Carlsbad, CA) according to the manufacturer's instructions.

Cell lysis, two-dimensional electrophoresis (2-DE), and Western blot

Cells were lysed on ice for 30 min in RIPA lysis buffer [50 mM Tris–HCl, pH 7.4, 150 mM NaCl, 2 mM EDTA, 0.1% SDS, 0.5% deoxycholate, 1% Nonidet P-40, 2 mM NaF, and protease inhibitor cocktail (Roche Applied Science, Germany)] and clarified at 12,000×*g* for 20 min. Protein concentrations were determined by Bradford assay (Bio-Rad, Hercules, CA). 2-DE was performed as previously described (Yang et al. 2006) using 7-cm Immobiline™ Dry Strips, pH 3–10NL or pH 3–5.6NL (Amersham Biosciences, Piscataway, NJ). For Western blotting, proteins were transferred onto nitrocellulose membranes (Amersham Biosciences) after SDS-polyacrylamide electrophoresis (PAGE) and further analyzed as previously described (Yang et al. 2008). Specific spots were visualized using enhanced chemiluminescence (Amersham Biosciences).

Succinylated wheat germ agglutinin (sWGA) lectin precipitation, immunoprecipitation, and in vitro binding assay

Protein samples were gently mixed with agarose-conjugated sWGA (Vector Laboratories, Burlingame, CA) or primary antibody and Protein A Sepharose™ CL-4B (Amersham Biosciences) for 2 h at 4°C. Precipitates were washed four times with lysis buffer, eluted with 1% SDS, and subjected to 2-DE. For FLAG- or Myc-tagged tubulin, an EZview™ Red Anti-FLAG M2 Affinity Gel (F 2426, Sigma) or an agarose-conjugated Myc antibody (sc-40AC, Santa Cruz Biotechnology) was used, and immunoprecipitates were eluted by boiling in 2× SDS sample buffer and resolved by SDS-PAGE. For in vitro binding assays, immunoprecipitates were incubated with protein samples for 2 h at 4°C and washed as above. For denaturing conditions, protein samples were adjusted to final concentrations of 0.5% SDS and 5 mM DTT and boiled for 3 min as previously described (Gambetta et al. 2009). Samples were then diluted five times with NET lysis buffer (50 mM Tris–HCl, pH 7.4, 150 mM NaCl, 2 mM EDTA, 1% Nonidet P-40) and processed for further experiments.

Mass spectrometric analysis

Specific protein spots excised from the Coomassie Brilliant Blue (CBB)-stained gel were digested with trypsin (Promega, Madison, WI) overnight at 37°C. For α- and β-tubulin digestion, Asp-N (Roche Applied Science) and chymotrypsin (Roche Applied Science) were used per the manufacturer's instructions. The resulting peptides were extracted with 50% acetonitrile and dried in a Speed Vac for further analysis. Mass spectrometry (MS) analysis was performed on a QSTAR Pulsar Q-TOF MS (Applied Biosystems), equipped with a nano-electrospray ion sources (Protana, Odense, Denmark) for peptide sequencing as described previously (Yang et al. 2006).

Measurement of soluble and assembled tubulin

Separation between soluble and assembled tubulin was performed as previously described (Minotti et al. 1991; Wang et al. 2006). Briefly, cells were rinsed twice with phosphate-buffered saline at room temperature and lysed with taxol-containing microtubule stabilizing buffer [20 mM Tris–HCl, pH 6.8, 140 mM NaCl, 0.5% Nonidet P-40, 1 mM $MgCl_2$, 2 mM EGTA, and 5 μM taxol (paclitaxel)]. After centrifugation at 12,000×*g* and 4°C, supernatants containing soluble tubulin were transferred into a new tube, and pellets containing polymerized tubulin were rinsed with lysis buffer and combined with cytoskeletal remains collected in 1% SDS from the corresponding wells. DNA was sheared by sonication. Equal portions (e.g., 1%) of each fraction were subjected to SDS-PAGE.

Measurement of neurite length

MN9D cells were plated onto 25 μg/ml poly-D-lysine-coated 100-mm dishes and maintained in culture medium for 3 days in the presence or absence of the indicated drug. Cells from five to ten randomly selected areas were photographed using an Axiovert phase-contrast microscope equipped with an Axiocam digital camera. Quantification of neurite lengths was performed using an Axiovision Image Analyzer (Carl Zeiss, Zena, Germany) as previously described (Eom et al. 2005).

Statistical analysis

Compiled data are expressed as mean ± SD. We used the two-tailed Student's *t* test for statistical analysis (*$P < 0.05$, **$P < 0.01$, and ***$P < 0.001$).

Results

O-GlcNAcylation of tubulin exist in MN9D neuronal cells

To examine whether *O*-GlcNAc modifications change during neuronal differentiation, undifferentiated MN9D

cells were treated with tRA for 3 days. 70–80% of MN9D cells undergo morphological changes at 2 days, and the total extent of neurites per cell reaches at 85–100 μm at day 3 (Castro et al. 2001; Eom et al. 2005). As expected, tRA-treated cells extended neurites as shown in Fig. 1a. To detect *O*-GlcNAcylation, cellular lysates of control and tRA-treated cells were subjected to 2-DE and then analyzed by Western blotting with an anti-*O*-GlcNAc antibody (CTD110.6). As shown in Fig. 1b, total *O*-GlcNAcylation patterns of MN9D cells were altered during differentiation; some protein *O*-GlcNAcylation spots appeared to increase while others seemed to decrease. To examine the function of *O*-GlcNAcylation in neuronal cells, we identified *O*-GlcNAcylated proteins from MN9D cells using agarose-conjugated sWGA, which is a specific lectin for GlcNAc. The sWGA precipitates were subjected to 2-DE, and protein spots were identified by MS (Fig. 1c). We found several potentially *O*-GlcNAcylated proteins, including α- and β-tubulin (Table 1).

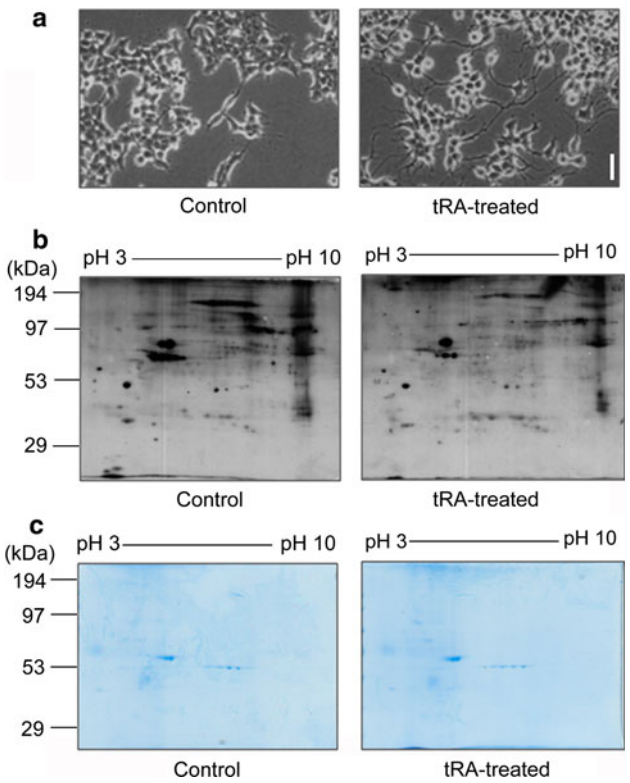

Fig. 1 Nucleocytoplasmic *O*-GlcNAcylation is dynamically altered during tRA-induced neuronal cell differentiation. **a** MN9D cells were treated with tRA for 3 days, and the phase-contrast images were obtained using an Axiovert microscope (Carl Zeiss, Jena, Germany) (*scale bar* 50 μm). **b** Cellular *O*-GlcNAc modification patterns were analyzed by 2-DE and Western blotting using an anti-*O*-GlcNAc antibody. **c** *O*-GlcNAc modified proteins were precipitated using agarose-conjugated sWGA and analyzed by 2-DE. Proteins were stained with CBB, and the visible protein spots were identified using ESI Q-TOF mass spectrometry

To confirm that α- and β-tubulin are modified with *O*-GlcNAc, we performed an immunoprecipitation assay with anti-α- and β-tubulin antibodies. Because the molecular weight of the immunoglobulin heavy chain (IgG HC) is similar to that of tubulin, α- and β-tubulin were separated from IgG HC by 2-DE and analyzed by Western blotting with an anti-*O*-GlcNAc antibody. Both α- and β-tubulin were detected as four spots and modified with *O*-GlcNAc (Fig. 2). α- and β-tubulin are distinguishable from each other because the theoretical isoelectric points (p*I*s) of the α- and β-tubulin isotypes are in the range of pH 4.94–4.98 and pH 4.78–4.82, respectively.

All tubulin isotypes found in MN9D neuronal cells are *O*-GlcNAcylated

We further examined which tubulin isotype is *O*-GlcNAcylated. α-Tubulin has six isotypes and β-tubulin has seven isotypes in vertebrates, which are differentially expressed both temporally and spatially. Therefore, we synthesized cDNA from MN9D cells and amplified the tubulin genes by PCR using tubulin isotype-specific primers. Four α-tubulin isotypes (α1, α1b, α1c, and α4) and four β-tubulin isotypes (β2b, β2c, β3, and β6) were cloned into FLAG- and Myc-tagged vectors, respectively. These tubulin isotypes were then co-expressed with OGT in HEK293 cells and immunoprecipitated with either an anti-FLAG or an anti-Myc antibody. Western blotting with an anti-*O*-GlcNAc antibody revealed that all tubulin isotypes were modified with *O*-GlcNAc (Fig. 3), although the tubulin isotypes differed at some amino acid sequences, especially at the C-terminus. These results suggest that differences in isotypes do not affect recognition by OGT.

O-GlcNAcylated peptides of tubulin are detectable by MS

Next, we investigated the *O*-GlcNAc site(s) on both α- and β-tubulin. α-Tubulin (α1b) and β-tubulin (β3) were co-expressed with OGT in HEK293 cells and immunoprecipitated with an anti-FLAG or an anti-Myc antibody, respectively. The immunoprecipitates were subjected to SDS-PAGE and visualized with CBB staining. Tubulin bands were excised from the gel and digested with both Asp-N and chymotrypsin. The extracted peptides were analyzed using ESI Q-TOF, and the *O*-GlcNAc peptides were recognized by GlcNAc oxonium ion scanning. We identified one *O*-GlcNAcylated peptide of α-tubulin 173–185 (PAPQVSTAVVEPY; Fig. 4a) and two *O*-GlcNAcylated peptides of β-tubulin 216–233 (KLATPTY GDLNHLVSATM; data not shown) and 224–238 (DLN HLVSATMSGVTT; Fig. 4b). These regions are conserved

Table 1 Potential *O*-GlcNAcylated proteins in MN9D cells

Protein name	Accession #	Mascot score	Matched peptide	*O*-GlcNAc description
Nuclear pore complex glycoprotein p62	gil1083437	752	27	Lubas et al. (1995)
Nucleoporin 54	gil39930543	653	14	Wells et al. (2002)
C1 transcription factor	gil4098678	366	12	Khidekel et al. (2004)
α-Tubulin isotype M-alpha-2	gil202210	364	11	Walgren et al. (2003)
PLIC-2	gil6014493	224	6	
Y box transcription factor	gil199821	147	5	Wang et al. (2007)
Tubulin, beta, 2	gil13542680	124	4	Wang et al. (2007)
Psmd11 protein	gil20988514	70	2	
Ddhd2 protein	gil28374267	63	2	
p120	gil53545	61	3	

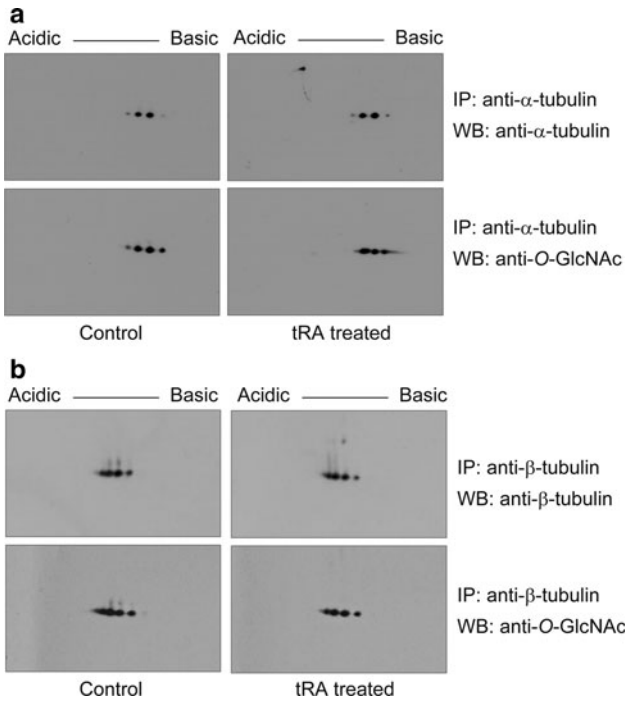

Fig. 2 Tubulin *O*-GlcNAcylation is confirmed using immunoprecipitation and Western blotting. Either α- or *β*-tubulin was purified from MN9D cells using an anti-α- or an anti-*β*-tubulin antibody, respectively. The immunoprecipitates were analyzed by 2-DE and Western blotting using an anti-*O*-GlcNAc antibody. **a** α-Tubulin was detected as four spots and modified with *O*-GlcNAc. **b** *β*-Tubulin was detected as four spots and modified with *O*-GlcNAc

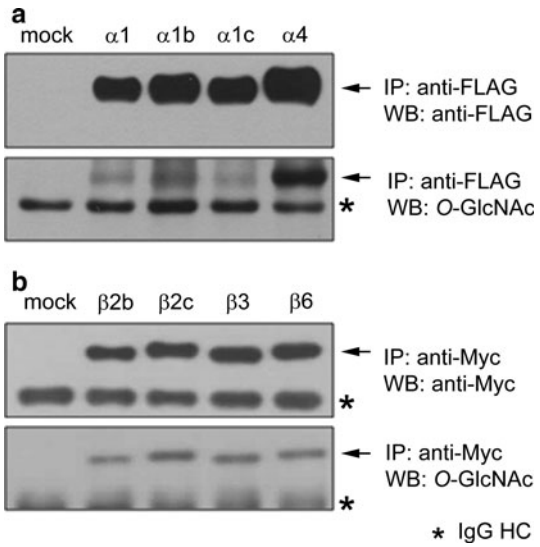

Fig. 3 *O*-GlcNAcylation occurs in all tubulin isotypes found in MN9D cells. Both α- and *β*-tubulin isotypes were cloned from MN9D cells, co-expressed with OGT in HEK293 cells, and analyzed by immunoprecipitation and Western blotting. **a** FLAG-tagged α-tubulin isotypes (α1, α1b, α1c, and α4) were purified and subjected to SDS-PAGE. Specific bands were detected by anti-FLAG and anti-*O*-GlcNAc antibodies (*black arrow*). **b** Myc-tagged *β*-tubulin isotypes (*β*2b, *β*2c, *β*3, and *β*6) were purified and subjected to SDS-PAGE. Specific bands were detected by anti-Myc and anti-*O*-GlcNAc antibodies (*black arrow*). FLAG- and Myc-tagged tubulins have higher molecular weights and are distinguishable from IgG HC (*asterisk*)

among the tubulin isotypes. The putative *O*-GlcNAc site of α-tubulin is either serine 178 or threonine 179, and these sites map to the GTP-binding and dimerization region. This result suggests that *O*-GlcNAcylation can affect tubulin heterodimerization. The *O*-GlcNAc sites of *β*-tubulin are one of the seven serine or threonine sites; however, we were unable to determine the specific residue where *O*-GlcNAcylation occurred.

O-GlcNAcylation on α-tubulin negatively regulates dimerization

To examine the function of the tubulin *O*-GlcNAcylation, we performed an in vitro binding assay. HEK293 cells were transfected with DNA construct encoding either FLAG-tagged α-tubulin or Myc-tagged *β*-tubulin. FLAG-tagged α-tubulin was expressed under conditions that increased intracellular *O*-GlcNAcylation after treatment of

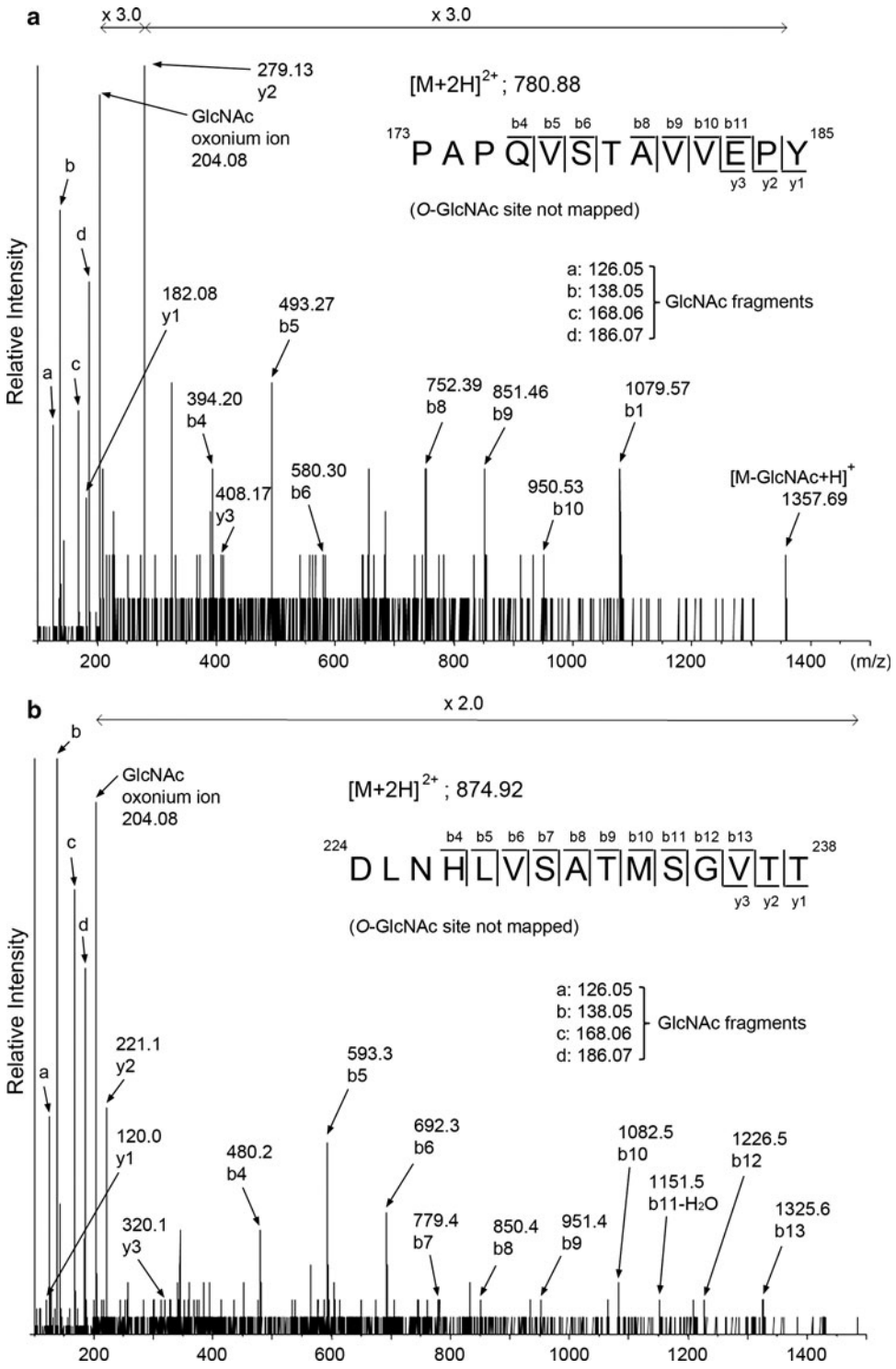

Fig. 4 *O*-GlcNAcylated peptides of tubulin were identified using mass spectrometry. FLAG-tagged α-tubulin (α1b) or Myc-tagged *β*-tubulin (*β*3) was co-expressed with OGT in HEK293 cells and immunoprecipitated using an anti-FLAG or an anti-Myc antibody, respectively. The immunoprecipitates were subjected to SDS-PAGE, and specific bands were excised from the gel. The α- and *β*-tubulin bands were digested with Asp-N and chymotrypsin simultaneously, and the extracted peptides were analyzed using ESI Q-TOF. *O*-GlcNAc bearing peptides from both α- and *β*-tubulin were detected by GlcNAc oxonium ion scanning. **a** The Q-TOF spectrum and sequencing results of an *O*-GlcNAc peptide of α-tubulin are shown. This peptide corresponds to residues 173–185 (PAPQVSTAVVEPY) at $[M + 2H]^{2+}$ *m/z* 780.88. **b** The Q-TOF spectrum and sequencing results of an *O*-GlcNAc peptide of *β*-tubulin are shown. This peptide corresponds to residues 224–238 (DLNHLVSATMSGVTT) at $[M + 2H]^{2+}$ *m/z* 874.92. However, *O*-GlcNAcylation sites were not precisely mapped

an OGA inhibitor or after OGT over-expression. After immunoprecipitation with an anti-FLAG antibody, FLAG-tagged α-tubulin was incubated with Myc-tagged *β*-tubulin. The precipitates were resolved by SDS-PAGE and analyzed by Western blotting with anti-FLAG and anti-Myc antibodies. The amount of Myc-tagged *β*-tubulin, which was bound to FLAG-tagged α-tubulin, was analyzed using densitometry. The amount of bound *β*-tubulin was decreased in response to the increased *O*-GlcNAcylation of α-tubulin (Fig. 5a). These results are consistent with the mass analysis data that the *O*-GlcNAcylation of α-tubulin occurs in the dimerization region.

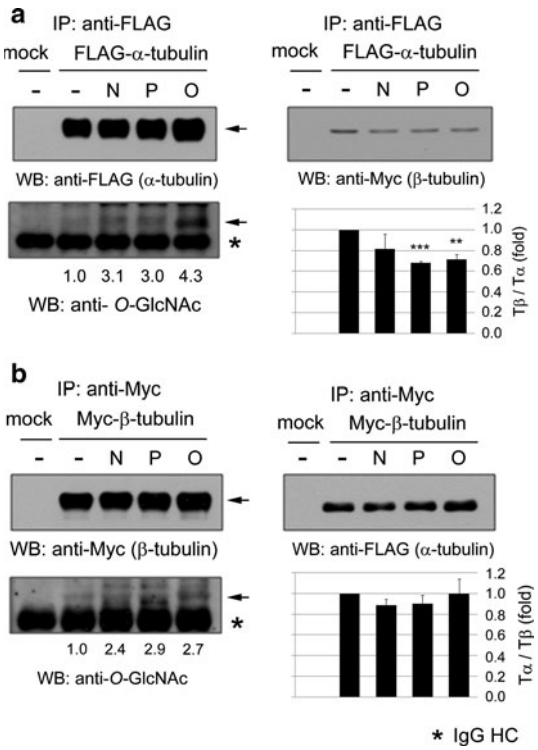

Fig. 5 *O*-GlcNAcylation on α-tubulin inhibits its interaction with *β*-tubulin, but *O*-GlcNAcylation on *β*-tubulin does not. An in vitro binding assay for α-tubulin (α1b) and *β*-tubulin (*β*3) was performed. **a** FLAG-tagged α-tubulin (α1b) was expressed in HEK293 cells and, to increase intracellular *O*-GlcNAcylation, either an OGA inhibitor (NButGT or PUGNAc) was applied or OGT was over-expressed. After precipitation with anti-FLAG antibody-conjugated Sepharose CL-4B, FLAG-tagged α-tubulin precipitates were incubated with Myc-tagged *β*-tubulin expressed in HEK293 cells for 2 h at 4°C. The precipitates were subjected to SDS-PAGE and analyzed by Western blotting. Either OGA inhibitor treatment or OGT over-expression increased tubulin *O*-GlcNAcylation. The increase in tubulin *O*-GlcNAcylation compared to un-treated (–) is indicated by a fold change under each lane of the blot. The amount of Myc-tagged *β*-tubulin that was bound to FLAG-tagged α-tubulin was analyzed using densitometry. The values were normalized to FLAG-tagged α-tubulin. The results of the *upper panel* are presented as mean ± SD (**$P < 0.01$ and ***$P < 0.001$). **b** Myc-tagged *β*-tubulin (*β*3) was expressed in HEK293 cells and purified using anti-Myc antibody-conjugated Sepharose CL-4B. Myc-tagged *β*-tubulin precipitates were then incubated with FLAG-tagged α-tubulin expressed in HEK293 cells for 2 h at 4°C. The precipitates were subjected to SDS-PAGE and analyzed by Western blotting. The amount of FLAG-tagged α-tubulin that was bound to Myc-tagged *β*-tubulin was analyzed using densitometry. *N* NButGT, *P* PUGNAc, *O* OGT over-expressed

We performed a reverse, in vitro binding assay; Myc-tagged *β*-tubulin was expressed under conditions that increased intracellular *O*-GlcNAcylation. The amount of FLAG-tagged α-tubulin that was bound to Myc-tagged *β*-tubulin was analyzed using densitometry. In contrast to α-tubulin, the increase in *O*-GlcNAcylation of *β*-tubulin did not affect its interaction with α-tubulin (Fig. 5b).

O-GlcNAcylated tubulin does not incorporate into microtubules

To explore the influence of tubulin *O*-GlcNAcylation on microtubule formation, we separated tubulin into soluble and assembled pools. Using taxol-containing microtubule stabilizing buffer, assembled tubulin remained as microtubules during cell lysis. After the removal of the soluble fraction, microtubules and other cytoskeletal proteins were collected in 1% SDS-dissociation buffer. We first examined the distribution of *O*-GlcNAcylated tubulin by sWGA precipitation. To prevent the precipitation of unmodified proteins that interact with *O*-GlcNAcylated proteins, we denatured the protein samples prior to sWGA precipitation. The purified proteins were then subjected to SDS-PAGE, and *O*-GlcNAcylated tubulin was detected by an anti-α- or an anti-*β*-tubulin antibody. As shown in Fig. 6a, *O*-GlcNAcylated α-tubulin was detected only in the soluble fraction, which suggests that *O*-GlcNAcylated α-tubulin does not incorporate into microtubules. This result is consistent with our finding that *O*-GlcNAcylated α-tubulin seemed to disturb *α*/*β*-tubulin heterodimerization. Interestingly, *O*-GlcNAcylated *β*-tubulin was absent in the assembled fraction (Fig. 6b), in which *O*-GlcNAcylation did not affect heterodimer formation.

OGA inhibitor treatment reduces neurite outgrowth

Next, we investigated whether tubulin *O*-GlcNAcylation affects neurite extension. Neurite outgrowth is largely dependent on microtubule polymerization. To increase cellular *O*-GlcNAcylation levels, we treated cells with an OGA inhibitor, NButGT or PUGNAc. Co-treatment of cells with OGA inhibitor and tRA resulted in an increase in intracellular *O*-GlcNAcylation and a decrease in neurite outgrowth. Neurite length was measured using an Axiovision Image Analyzer, and relative neurite length decreased by 20% compared to tRA only-treated MN9D cells (Fig. 7). These results indicate that the increase in the amount of *O*-GlcNAcylated tubulin reduced microtubule formation and resulted in decreased neurite outgrowth.

Discussion

In this study, we demonstrate that tubulin *O*-GlcNAcylation negatively regulates microtubule formation. We found that both α- and *β*-tubulin were modified with *O*-GlcNAc in MN9D neuronal cells and that tubulin *O*-GlcNAcylation occurred regardless of tubulin isotype. We identified *O*-GlcNAcylated peptides from both α- and *β*-tubulin, and *O*-GlcNAc sites were located near the nucleotide-binding region. In addition, *O*-GlcNAcylated tubulin appeared to

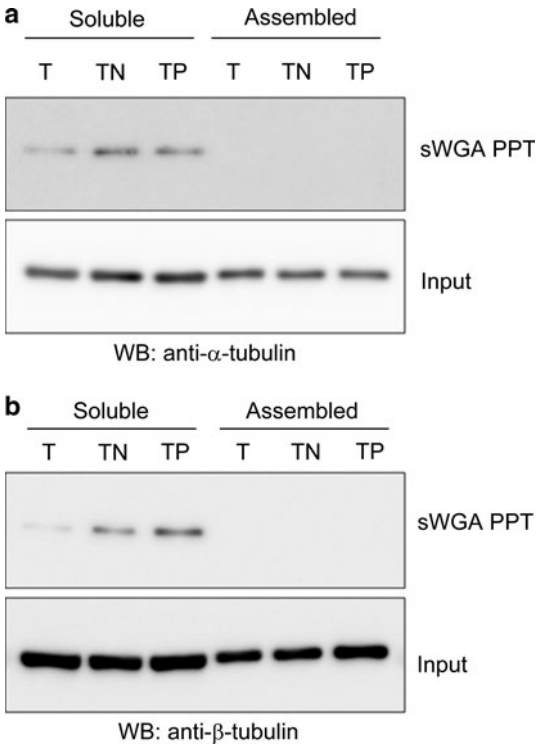

Fig. 6 *O*-GlcNAcylated tubulin is found in the soluble fraction but not in the assembled fraction. Tubulin from MN9D cells was separated into soluble and assembled fractions using taxol-containing microtubule stabilizing buffer as described in "Materials and Methods". Each fraction was denatured by boiling for 3 min in 0.5% SDS and 5 mM DTT. The same amount (1%) of each fraction was preserved as input. After a fivefold dilution with NET buffer, protein samples were incubated with agarose-bound sWGA. The sWGA precipitates (PPT) were subjected to SDS-PAGE, and α- and β-tubulin were detected by Western blotting. **a** α-Tubulin was separated into soluble and assembled fractions and *O*-GlcNAcylated α-tubulin was detected in the soluble fraction. **b** β-Tubulin was separated into soluble and assembled fractions and *O*-GlcNAcylated β-tubulin was detected in the soluble fraction. *T* tRA, *N* NButGT, *P* PUGNAc

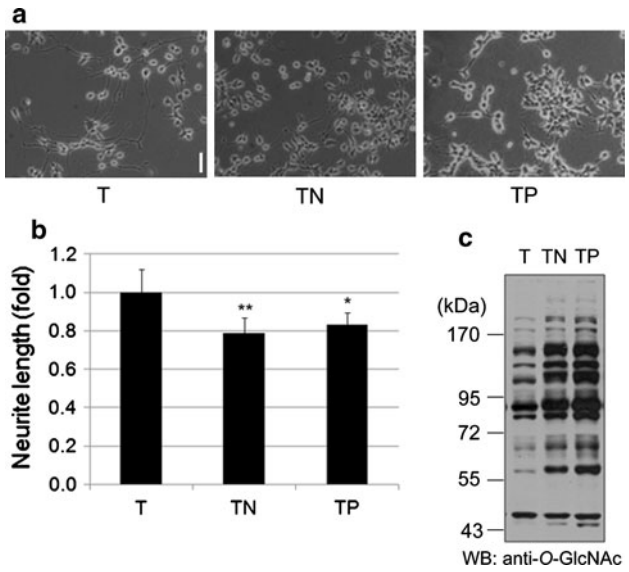

Fig. 7 *O*-GlcNAcase inhibitor treatment reduces neurite outgrowth of MN9D cells. **a** The phase-contrast images of tRA-treated or tRA and *O*-GlcNAcase inhibitor co-treated MN9D cells were taken on day 3 (*scale bar* 50 μm). **b** Neurite length was measured using an Axiovision Image Analyzer, and relative neurite length of tRA and NButGT or PUGNAc co-treated samples decreased by 20 and 17%, respectively. The data are presented as mean ± SD ($*P < 0.05$ and $**P < 0.01$). **c** Total cellular *O*-GlcNAcylation was examined by Western blotting using an anti-*O*-GlcNAc antibody. *T* tRA, *N* NButGT, *P* PUGNAc

be unable to assemble into microtubules, and the increase in *O*-GlcNAcylation diminished tRA-induced neurite outgrowth in MN9D cells.

Various tubulin PTMs have been reported, but most are located in the C-terminal region of tubulin and occur in stable microtubules. Polyglycylation and polyglutamylation occur on α- and β-tubulin in the axonemes of both cilia and flagella (Edde et al. 1990; Redeker et al. 1994) and in the axons of neuronal cells (Audebert et al. 1994). The C-terminal region of tubulin is located on the outer surfaces of the microtubules and is important for protein–protein interactions, including those involving motor proteins and MAPs. However, α/β-tubulin lacking the C-terminal region still assembles into microtubules.

There are few reports of PTMs on the other regions of tubulin. The Cdk1/cyclin B complex, which is required for mitotic entry, phosphorylates serine 172 of β-tubulin during mitosis. And phosphorylated β-tubulin does not polymerized into microtubules (Fourest-Lieuvin et al. 2006). The serine 172 residue is located in the GTP-binding site of β-tubulin, which interacts with α-tubulin within microtubules. In our study, α-tubulin *O*-GlcNAcylation occurred on either serine 178 or threonine 179 residue, and inhibited α/β heterodimerization. These residues are also located in the GTP-binding site, which interacts with β-tubulin to form α/β heterodimer. It is possible that *O*-GlcNAcylation on α-tubulin results in steric hindrance effects on heterodimerization. Taken together, β-tubulin phosphorylation and α-tubulin *O*-GlcNAcylation are thought to be important regulatory modifications for microtubule dynamics.

Our finding that *O*-GlcNAcylation on α-tubulin inhibits dimer formation can be explained by the tubulin heterodimerization process, which is regulated by several factors, including tubulin-binding cofactor (TBC) A–E. Newly synthesized α- and β-tubulin monomers are known to be captured by TBC-E and TBC-D, respectively. TBC-E-bound α-tubulin and TBC-D-bound β-tubulin can interact with each other and then form a multimeric complex. TBC-C then associates with this complex and activates the GTPase activity of β-tubulin, resulting in the release of the α/β-tubulin heterodimer from the complex (Tian et al. 1997; Cowan and Lewis 2001). Conversely, each molecule

of TBC-D and TBC-E can interact with the α/β-tubulin heterodimer, and, consequently, tubulin dimer interaction is disrupted (Bhamidipati et al. 2000). This mechanism allows the α/β-tubulin heterodimer to exchange partners. Under these circumstances, TBC-E-bound α-tubulin can be modified with *O*-GlcNAc, resulting in a loss of ability to interact with β-tubulin.

We found that β-tubulin *O*-GlcNAcylation occurs on residues 216–233 (KLATPTYGDLNHLVSATM) and 224–238 (DLNHLVSATMSGVTT). There are five threonine and two serine residues in this region, and serine 230 and threonine 232 are common in these *O*-GlcNAcylated peptides. It is possible that one of these two residues is the *O*-GlcNAcylation site of β-tubulin. However, there might be another *O*-GlcNAcylation site on a non-overlapping residue. In the 3D structure of β-tubulin, this region forms α-helix H7, which is located between the nucleotide-binding and taxol-binding sites. *O*-GlcNAcylation in this region may alter the structure slightly. Therefore, *O*-GlcNAcylated β-tubulin might be unable to exchange GDP for GTP, which is required for polymerization.

Tubulin *O*-GlcNAcylation is thought to have a low stoichiometry (Hart et al. 2007), raising concerns about its influence on microtubule function. However, we did not find *O*-GlcNAcylated tubulin in microtubules. Roughly, one half of the total tubulin appears to exist as heterodimers (Minotti et al. 1991), and microtubule polymerization occurs more dynamically at the plus ends than at the minus ends (Howard and Hyman 2003). It is possible that both OGT and OGA associate at the plus ends of the microtubules and regulate the *O*-GlcNAc modification of the α/β-tubulin heterodimer. In contrast, other PTMs, which occur in stable microtubules, do not affect the dynamic behavior of the microtubules. It seems reasonable that tubulin *O*-GlcNAcylation occurs at a low level for its proper function.

In our study, *O*-GlcNAcylated β-tubulin was not found in microtubules, but still formed heterodimers. However, these results do not exclude the possibility that tubulin *O*-GlcNAcylation can result in the depolymerization of microtubules. In mature neurons, neurofilaments (NFs) are major components of the cytoskeleton. NF-H, -M, and -L are modified with *O*-GlcNAc at the N-terminal head domain, which is thought to regulate polymerization (Dong et al. 1993, 1996; Al-Chalabi and Miller 2003). Under conditions of glucose deprivation, p38 MAPK is activated and recruits OGT to NF-H; *O*-GlcNAcylation on NF-H then results in its depolymerization (Cheung and Hart 2008). Although the detailed depolymerization mechanism of NF-H might be different from that of tubulin, abnormally increased levels of *O*-GlcNAcylation on NFs and microtubules could negatively affect axonal structure and neuronal cell polarity in the brain.

In addition, microtubules are one of the most important players in the cell cycle. Microtubules form mitotic spindles during prophase and the midbody during telophase in mitosis. Abnormal *O*-GlcNAc modifications have been reported to delay in G2/M progression and alter mitotic phosphorylation and cyclin expression levels (Slawson et al. 2005). In addition, OGA over-expression disrupts the tubulin network and causes cells to form a round shape. OGT co-localizes with tubulin in the spindle and midbody, and cells that over-express OGT fail to undergo cytokinesis. Therefore, dysregulation of tubulin *O*-GlcNAcylation could disrupt the proper function of microtubules.

In conclusion, our findings that *O*-GlcNAcylated tubulin is excluded from microtubules suggest an important role of *O*-GlcNAcylation in the regulation of microtubules. Previous studies have shown that *O*-GlcNAcylation is involved in many disease states, including diabetes, neurodegenerative disorders, and cancer. We postulate that the dysregulation of tubulin *O*-GlcNAcylation is related to microtubule dysfunction in these diseases. Further verification of this hypothesis would enhance our understanding of microtubule function.

Acknowledgments This work was supported by grants from National Research Foundation funded by the Ministry of Education, Science and Technology Grant (R0A-2007-000-20011-0), and WCU project (R31-2008-000-10086-0). In addition, S.J., S.Y.P. and J.G.K. are fellowship awardees of the Brain Korea 21 program. This work was made possible through the use of research facilities in the Yonsei Center for Biotechnology.

References

Al-Chalabi A, Miller CC (2003) Neurofilaments and neurological disease. Bioessays 25:346–355

Arnold CS, Johnson GV, Cole RN, Dong DL, Lee M, Hart GW (1996) The microtubule-associated protein tau is extensively modified with *O*-linked *N*-acetylglucosamine. J Biol Chem 271:28741–28744

Audebert S, Koulakoff A, Berwald-Netter Y, Gros F, Denoulet P, Edde B (1994) Developmental regulation of polyglutamylated alpha- and beta-tubulin in mouse brain neurons. J Cell Sci 107(Pt 8):2313–2322

Baas PW (1997) Microtubules and axonal growth. Curr Opin Cell Biol 9:29–36

Bhamidipati A, Lewis SA, Cowan NJ (2000) ADP ribosylation factor-like protein 2 (Arl2) regulates the interaction of tubulin-folding cofactor D with native tubulin. J Cell Biol 149:1087–1096

Castro DS, Hermanson E, Joseph B, Wallen A, Aarnisalo P, Heller A, Perlmann T (2001) Induction of cell cycle arrest and morphological differentiation by Nurr1 and retinoids in dopamine MN9D cells. J Biol Chem 276:43277–43284

Cheung WD, Hart GW (2008) AMP-activated protein kinase and p38 MAPK activate *O*-GlcNAcylation of neuronal proteins during glucose deprivation. J Biol Chem 283:13009–13020

Choi HK, Won LA, Kontur PJ, Hammond DN, Fox AP, Wainer BH, Hoffmann PC, Heller A (1991) Immortalization of embryonic

mesencephalic dopaminergic neurons by somatic cell fusion. Brain Res 552:67–76

Chou CF, Smith AJ, Omary MB (1992) Characterization and dynamics of *O*-linked glycosylation of human cytokeratin 8 and 18. J Biol Chem 267:3901–3906

Conde C, Caceres A (2009) Microtubule assembly, organization and dynamics in axons and dendrites. Nat Rev Neurosci 10:319–332

Cowan NJ, Lewis SA (2001) Type II chaperonins, prefoldin, and the tubulin-specific chaperones. Adv Protein Chem 59:73–104

Ding M, Vandre DD (1996) High molecular weight microtubule-associated proteins contain *O*-linked-*N*-acetylglucosamine. J Biol Chem 271:12555–12561

Dong DL, Xu ZS, Chevrier MR, Cotter RJ, Cleveland DW, Hart GW (1993) Glycosylation of mammalian neurofilaments. Localization of multiple *O*-linked *N*-acetylglucosamine moieties on neurofilament polypeptides L and M. J Biol Chem 268: 16679–16687

Dong DL, Xu ZS, Hart GW, Cleveland DW (1996) Cytoplasmic *O*-GlcNAc modification of the head domain and the KSP repeat motif of the neurofilament protein neurofilament-H. J Biol Chem 271:20845–20852

Edde B, Rossier J, Le Caer JP, Desbruyeres E, Gros F, Denoulet P (1990) Posttranslational glutamylation of alpha-tubulin. Science 247:83–85

Eom DS, Choi WS, Ji S, Cho JW, Oh YJ (2005) Activation of c-Jun N-terminal kinase is required for neurite outgrowth of dopaminergic neuronal cells. Neuroreport 16:823–828

Fourest-Lieuvin A, Peris L, Gache V, Garcia-Saez I, Juillan-Binard C, Lantez V, Job D (2006) Microtubule regulation in mitosis: tubulin phosphorylation by the cyclin-dependent kinase Cdk1. Mol Biol Cell 17:1041–1050

Gambetta MC, Oktaba K, Muller J (2009) Essential role of the glycosyltransferase sxc/Ogt in polycomb repression. Science (New York, NY) 325:93–96

Gordon-Weeks PR (2004) Microtubules and growth cone function. J Neurobiol 58:70–83

Hammond JW, Cai D, Verhey KJ (2008) Tubulin modifications and their cellular functions. Curr Opin Cell Biol 20:71–76

Hart GW, Housley MP, Slawson C (2007) Cycling of *O*-linked beta-*N*-acetylglucosamine on nucleocytoplasmic proteins. Nature 446:1017–1022

Howard J, Hyman AA (2003) Dynamics and mechanics of the microtubule plus end. Nature 422:753–758

Kang JG, Park SY, Ji S, Jang I, Park S, Kim HS, Kim SM, Yook JI, Park YI, Roth J, Cho JW (2009) *O*-GlcNAc protein modification in cancer cells increases in response to glucose deprivation through glycogen degradation. J Biol Chem 284:34777–34784

Khidekel N, Ficarro SB, Peters EC, Hsieh-Wilson LC (2004) Exploring the *O*-GlcNAc proteome: direct identification of *O*-GlcNAc-modified proteins from the brain. Proc Natl Acad Sci USA 101:13132–13137

Ku NO, Omary MB (1994) Expression, glycosylation, and phosphorylation of human keratins 8 and 18 in insect cells. Exp Cell Res 211:24–35

Liu F, Iqbal K, Grundke-Iqbal I, Hart GW, Gong CX (2004) *O*-GlcNAcylation regulates phosphorylation of tau: a mechanism involved in Alzheimer's disease. Proc Natl Acad Sci USA 101:10804–10809

Love DC, Hanover JA (2005) The hexosamine signaling pathway: deciphering the "*O*-GlcNAc code". Sci STKE 2005:re13

Lubas WA, Smith M, Starr CM, Hanover JA (1995) Analysis of nuclear pore protein p62 glycosylation. Biochemistry 34:1686–1694

Mandell JW, Banker GA (1995) The microtubule cytoskeleton and the development of neuronal polarity. Neurobiol Aging 16:229–237 (discussion 238)

Marshall S, Nadeau O, Yamasaki K (2004) Dynamic actions of glucose and glucosamine on hexosamine biosynthesis in isolated adipocytes: differential effects on glucosamine 6-phosphate, UDP-*N*-acetylglucosamine, and ATP levels. J Biol Chem 279:35313–35319

Minotti AM, Barlow SB, Cabral F (1991) Resistance to antimitotic drugs in Chinese hamster ovary cells correlates with changes in the level of polymerized tubulin. J Biol Chem 266:3987–3994

Redeker V, Levilliers N, Schmitter JM, Le Caer JP, Rossier J, Adoutte A, Bre MH (1994) Polyglycylation of tubulin: a posttranslational modification in axonemal microtubules. Science 266:1688–1691

Slawson C, Zachara NE, Vosseller K, Cheung WD, Lane MD, Hart GW (2005) Perturbations in *O*-linked beta-*N*-acetylglucosamine protein modification cause severe defects in mitotic progression and cytokinesis. J Biol Chem 280:32944–32956

Slawson C, Lakshmanan T, Knapp S, Hart GW (2008) A mitotic GlcNAcylation/phosphorylation signaling complex alters the posttranslational state of the cytoskeletal protein vimentin. Mol Biol Cell 19:4130–4140

Tian G, Lewis SA, Feierbach B, Stearns T, Rommelaere H, Ampe C, Cowan NJ (1997) Tubulin subunits exist in an activated conformational state generated and maintained by protein cofactors. J Cell Biol 138:821–832

Verhey KJ, Gaertig J (2007) The tubulin code. Cell Cycle 6: 2152–2160

Walgren JL, Vincent TS, Schey KL, Buse MG (2003) High glucose and insulin promote *O*-GlcNAc modification of proteins, including alpha-tubulin. Am J Physiol 284:E424–E434

Wang Y, Tian G, Cowan NJ, Cabral F (2006) Mutations affecting beta-tubulin folding and degradation. J Biol Chem 281: 13628–13635

Wang Z, Pandey A, Hart GW (2007) Dynamic interplay between *O*-linked *N*-acetylglucosaminylation and glycogen synthase kinase-3-dependent phosphorylation. Mol Cell Proteomics 6:1365–1379

Wells L, Vosseller K, Cole RN, Cronshaw JM, Matunis MJ, Hart GW (2002) Mapping sites of *O*-GlcNAc modification using affinity tags for serine and threonine post-translational modifications. Mol Cell Proteomics 1:791–804

Westermann S, Weber K (2003) Post-translational modifications regulate microtubule function. Nat Rev Mol Cell Biol 4:938–947

Yang WH, Kim JE, Nam HW, Ju JW, Kim HS, Kim YS, Cho JW (2006) Modification of p53 with *O*-linked *N*-acetylglucosamine regulates p53 activity and stability. Nat Cell Biol 8:1074–1083

Yang WH, Park SY, Nam HW, Kim do H, Kang JG, Kang ES, Kim YS, Lee HC, Kim KS, Cho JW (2008) NFkappaB activation is associated with its *O*-GlcNAcylation state under hyperglycemic conditions. Proc Natl Acad Sci USA 105:17345–17350

Yang WH, Park SY, Ji S, Kang JG, Kim JE, Song H, Mook-Jung I, Choe KM, Cho JW (2010) *O*-GlcNAcylation regulates hyperglycemia-induced GPX1 activation. Biochem Biophys Res Commun 391:756–761

Zachara NE, O'Donnell N, Cheung WD, Mercer JJ, Marth JD, Hart GW (2004) Dynamic *O*-GlcNAc modification of nucleocytoplasmic proteins in response to stress A survival response of mammalian cells. J Biol Chem 279:30133–30142